

On the Molecular-Beam Epitaxy of Topological Insulator Bi_2Se_3 (111) and (221) Thin Films

Maohai Xie, Xin Guo, Zhongjie Xu, and Wingkin Ho

Physics Department, The University of Hong Kong, Pokfulam Road, Hong Kong

Abstract

This paper presents an overview of growth of Bi_2Se_3 , a prototypical three-dimensional topological insulator, by molecular-beam epitaxy on various substrates. Comparison is made between growths of Bi_2Se_3 (111) on van der Waals (vdW) and non-vdW types of substrates, with the attention paid on twin suppression and strain. Growth along the [221] direction of Bi_2Se_3 on InP(001) and GaAs(001) substrates is also discussed.

Keywords: topological insulator, MBE, Bi_2Se_3 , twin domain, strain

PACS: 81.15.-z, 81.10.-h, 68.55.-a, 68.37.-d,

1. Introduction

Characterizations of topological insulators (TIs) for their quantum properties demand high quality samples. Early experiments on surface electronic structures of the three-dimensional (3D) TIs were made on bulk crystals prepared by thermal cooling of stoichiometric melts, for example.^[1-4] Although such bulk samples exhibited good structural and electronic quality, they were not very suitable for transport studies. Consequently, effort has been increasingly directed towards growing TI thin film samples by epitaxial methods, such as molecular-beam epitaxy (MBE).^[5-20] Particularly, because of the ultrahigh vacuum condition of MBE, surface characterizations of the samples become viable during or immediately after the growth experiment, eliminating potential complications due to surface contamination by the ambient environment.^[2, 21] Moreover, thin film samples are particularly suitable for making gated device structures, essential for chemical potential tuning in transport experiments.^[10, 11, 15, 16, 22]

In this paper, we present an overview of some recent findings and results of MBE growth of Bi_2Se_3 compound, a prototypical 3D topological insulator.^[1, 23] We will pay particular attention to the general growth properties and elaborate on twin domain suppression and strain relaxation in epitaxial Bi_2Se_3 on different substrates. Growths of Bi_2Se_3 along both [111] and [221] directions will be discussed.

2. General growth properties

Bi_2Se_3 was among the first a few 3D topological insulators being discovered by theory and experiment (the others include Bi_2Te_3 and Sb_2Te_3).^[1, 23] Bi_2Se_3 is particularly attractive because it has a relatively large energy bandgap in its bulk (~ 0.3 eV), holding the promise of high temperature applications. Crystalline Bi_2Se_3 has the rhombohedral structure with the space group $R\bar{3}m$. It can be described also in terms of a hexagonal primitive cell containing three quintuple layers (QLs) of alternating selenium (Se) and bismuth (Bi) atoms stacked in the sequence of $-\text{[ABCAB]-[CABCA]-[BCABC]-}$ along the trigonal (c -) axis. Here $-\text{[...]-}$ denotes

one Bi_2Se_3 QL composed of two Bi atomic layers sandwiched between three Se layers. The atoms within each QL unit are chemically bonded, whereas those between adjacent QLs are bonded by the weak van der Waals (vdW) force. The “gap” between the vdW-force bonded atomic planes is a natural cleavage plane, which is readily obtained by cleavage of a bulk crystal or by growth of an epitaxial film. Such a plane, i.e., $\text{Bi}_2\text{Se}_3(111)$, is the only surface being extensively studied so far by surface techniques like angle resolved photoemission spectroscopy (ARPES) and scanning tunneling microscopy and spectroscopy (STM/STS),^[1, 2, 7, 8, 24] for example.

$\text{Bi}_2\text{Se}_3(111)$ has been found to grow readily on many different substrates with a wide variations of lattice constants. It reflects the nature of van der Waals epitaxy (vdWe)^[25, 26] of the material. The unique layered structure of Bi_2Se_3 in the c -axis direction makes two-dimensional (2D) nucleation and growth of the compound along $[111]$ favorable. Past experiments have unambiguously shown that the growth unit of Bi_2Se_3 is one QL, in which Se and Bi are strongly bonded.^[5, 6] If one uses a substrate that is inert in terms of chemical interaction with Bi_2Se_3 deposit, the heterointerface is of the vdW bonding and the growth follows the conventional vdWe process. Also because of the weak vdW bonding, growth of Bi_2Se_3 appears quite tolerant to the choice of the substrate. The many substrates that people have used in the literature include silicon (Si),^[5, 6, 17, 27] GaAs,^[9] InP,^[17, 19, 20] CdS,^[12, 16] graphene,^[28] CaF_2 ,^[18] sapphire,^[15] SrTiO_3 ,^[10] GaN and SiC,^[29] to name a few. All of these resulted in $\text{Bi}_2\text{Se}_3(111)$ films. The large variation in lattice misfits between Bi_2Se_3 and these substrates does not appear critical, although small lattice misfits do tend to bring about better quality films.^[16, 19, 20, 29] The lattice misfit strain may readily be accommodated at the vdW interface without invoking chemical-bond breaking. As will be shown later in this paper, the first QL Bi_2Se_3 deposited on a vdW type of substrate (e.g., Si:H) shows a lattice parameter indistinguishable from that of a bulk crystal according to in situ reflection high-energy electron diffraction (RHEED) measurements. On a non-vdW type of substrate (such as GaAs), the residual strain in the first QL Bi_2Se_3 appears greater.

Before moving to a description of the growth characteristics of Bi_2Se_3 on different substrates, we first comment on the MBE conditions appropriate for Bi_2Se_3 epitaxy. At vacuum levels of $10^{-7} - 10^{-10}$ torr, typical for Bi_2Se_3 MBE, the solid phase of stoichiometric Bi_2Se_3 is in equilibrium with the vapor phases of Bi and Se at relatively low temperatures.^[30] Experiments have shown that the optimal temperature of growth is in the range of 150 – 250 °C. In general, a higher temperature is favored for enhanced surface diffusion and thus smoother surface morphology. But at too high a temperature, the condensation becomes incomplete and should be avoided. As for the flux of Bi and Se sources, according to the phase diagram,^[30] one has to choose a Se flux that is in excess of stoichiometry (i.e., the flux ratio $\text{Se}:\text{Bi} > 3:2$). On the other hand, because the flux of Se generated from a conventional Knudsen cell is composed mainly of Se tetramers (Se_4), whose decomposition is not very efficient, a much higher Se flux, usually about 10 times or more than that of Bi, will be needed. If one has access to a cracker cell, Se dimers (Se_2) will be the main constituent in the vapor and a lower ratio between Se and Bi fluxes (e.g., $\text{Se}:\text{Bi} \sim 3:1$) can be accepted.^[18]

3. Bi_2Se_3 epitaxy on hexagonal symmetrical substrate surfaces

So far, the majority of epitaxial Bi_2Se_3 films are grown on substrate surfaces that possess the hexagonal lattice symmetry, such as the (111) surfaces of cubic or rhombohedral crystals or the (0001) surfaces of wurtzite compounds. Such choices of substrates are natural considering the same hexagonal lattice of $\text{Bi}_2\text{Se}_3(111)$. For the various substrates employed, one may make a distinction between those where there are no unsaturated dangling bonds of the surface atoms and are thus of the vdW type and those with dangling bonds (non-vdW type). Graphene and hydrogen (H) terminated Si (Si:H) obviously belong to the former category while clean $\text{InP}(111)\text{A}$ and sapphire (0001) are of the latter type. It is worthwhile to compare the growth behaviors on these two different categories of substrates. Furthermore, there are different lattice misfits for different

substrates. How the lattice misfit strain affects the growth properties of Bi_2Se_3 and how strain is relaxed during growth are also of scientific and practical relevance.

3.1 Bi_2Se_3 deposition on vdW substrates

A number of early MBE growth experiments of Bi_2Se_3 were done using Si(111) substrate due to the obvious reasons of its wide availability, low cost and mature processing technology. Being the most important semiconductor, Si has an in-plane lattice parameter that is not too far from that of Bi_2Se_3 (0.384 nm for Si versus 0.414 nm of Bi_2Se_3). However, clean Si(111) is (7×7) reconstructed with dangling unsaturated bonds. So upon Bi_2Se_3 deposition, Se atoms may react with surface Si forming SiSe_2 , for example.^[27, 31] If so, it will not favor van der Waals epitaxy of Bi_2Se_3 . Our experiments have shown that direct deposition of Bi_2Se_3 on clean Si(111) $-(7 \times 7)$ at elevated temperatures does not result in single crystalline epilayers, which is evidenced by a ring patterns in the RHEED, signaling a polycrystalline film.^[29] In order to facilitate a crystalline epilayer growth on Si(111), one thus has to modify the surface prior to Bi_2Se_3 deposition. A number of methods have been developed for Si surface treatment, including dosing the surface with a coverage of Bi for a β - $(\sqrt{3} \times \sqrt{3})$ reconstructed surface,^[5] depositing a thin InSe buffer,^[14] and exposing the surface to a flux of Se for a Se-terminated one,^[32] for example. For the latter, one must be careful to choose a right temperature so as to avoid SiSe_2 formation. In a previous study, we adopted a more parameter-tolerant method: depositing a thin amorphous Bi-Se buffer at a cryostat temperature (~ 100 K) followed by annealing and subsequent deposition at an elevated temperature of 520 K.^[6] We found the method was effective in producing crystalline Bi_2Se_3 films.

A more common and simple approach to passivate the dangling bonds on Si(111) is by H-atom termination, which can be achieved simply by dipping the Si wafer into hydrofluoric acid.^[33] The surface then becomes (1×1) structured instead of the (7×7) reconstruction of clean Si(111). Bi_2Se_3 growth on such a surface follows the vdWe process.^[25, 26] Fig. 1 presents a STM image of a Bi_2Se_3 sample grown on Si(111):H by direct deposition at 490 K.^[29] As is seen, the

surface is dominated by triangular mounds with the steps on mounds being single QL high (~ 1 nm). Such a morphology is characteristic of $\text{Bi}_2\text{Se}_3(111)$ films grown on flat substrate surfaces.^[6] The triangular shape of the mounds reflects the three-fold symmetry of Bi_2Se_3 crystal about the c -axis. Kinetically, it is produced by anisotropic growth rates of two inequivalent steps on surface that are rooted at the bonding characteristics of atoms at these steps.^[34]

In the following, we draw attention of the orientation of the triangular mounds in Fig. 1. One notes they are not aligned but oppositely oriented. Such oppositely oriented mounds represent a common feature in morphology of epitaxial Bi_2Se_3 on Si:H and other vdW substrates. It reflects the epifilm to contain twin domains. Indeed, the orientation of the triangular mounds signifies the stacking order of atoms in Bi_2Se_3 (Fig. 2). If the film is of single domain with uniform in-plane alignment, the mounds ought to be aligned in one and the same direction. The oppositely oriented mounds seen in Fig. 1 mean the coexistence of different stacking orders in the sample and thus a twinned film. A twinned film would be globally six-fold symmetrical about the surface normal, which can be verified by low-energy electron diffraction (LEED) measurements. This is shown in the inset of Figure 1. Twinning of epitaxial Bi_2Se_3 on a flat vdW substrate may be understood from the fact that there is a weak vdW interaction between Bi_2Se_3 and the substrate and so the *subsurface* layer of atoms in the substrate may not play a role in constraining the lattices of the deposit. If so, i.e., only the top surface layer with the six-fold lattice symmetry provides a guide for epitaxial Bi_2Se_3 , two equivalent stacking configurations in Bi_2Se_3 : ABCAB versus ACBAC will become equally probable giving rise to the twinned film (Fig. 2). One may tune the growth parameter to affect the domain size, however, twin defects on flat vdW substrates can hardly be eliminated so long as the growth proceeds in the 2D nucleation mode.

In order to suppress twin formation, one may “turn on” the guiding role of the subsurface layer(s) of the substrate by choosing a substrate that strongly interacts with Bi_2Se_3 deposit, so that the subsurface atoms are influential in determining the epitaxial alignment of the deposit. Alternatively, one may adopt a vicinal substrate on which there exist trains of steps. Atoms at step

edges have dangling bonds, favoring strong chemical interaction. Step-edge atoms will then effect on the stacking of epitaxial Bi_2Se_3 , promoting a single and substrate-lattice-aligned domain under the step-flow growth mode. Fig. 3 shows an example of a Bi_2Se_3 film grown on a vicinal $\text{Si}(111)$. Instead of triangular mounds, the surface is composed of terraces and steps. A single domain Bi_2Se_3 film can be inferred from the RHEED pattern shown in the inset of Fig. 3, where the diffraction spots (marked by yellow dots) are seen to be asymmetrically distributed.^[29] Twin suppression has brought about improved electronic properties of the material, which are exemplified by the reduced background doping and enhanced electron mobility.^[6, 20]

Another aspect of interests in the growth of Bi_2Se_3 on vdW substrates is the lattice misfit strain. With the facility of in situ RHEED, we can monitor in-plane lattice parameter evolution of the deposit in real-time. We find that upon Bi_2Se_3 deposition, a new set of diffraction pattern emerges in the background of a pattern from the substrate surface. An example is given in the inset of Fig. 4, obtained from growth on a flat $\text{Si}(111):\text{H}$. Measuring the spacing D between the two integer streaks and comparing it to D_{Si} , the value of Si substrate, we derive in-plane lattice parameter of the deposit at various stages of growth. As it happens, at the very early stage of deposition when the diffraction streaks corresponding to Bi_2Se_3 deposit just emerged, the measured in-plane lattice constant is found indistinguishable from that of a bulk Bi_2Se_3 crystal (green line and open circles in Fig. 4). Therefore the nucleation islands of Bi_2Se_3 on Si:H (and on other vdW substrates) appears strain-relieved. Such strain-free QL high Bi_2Se_3 islands on the vdW substrates would be consistent with the weak interaction between Bi_2Se_3 and the substrate at their interfaces and so Bi_2Se_3 epifilm can hardly be strained by the lattice of the substrate. However to our surprise, we find the lattice constant of the growing Bi_2Se_3 to continue to evolve with deposition coverage and reach a maximum of approximately 0.418 nm at ~ 1 QL before gradually recovers that of the bulk value of 0.414 nm. This is shown in Fig. 4. So there is $\sim 1\%$ lattice stretch over a bulk Bi_2Se_3 crystal at ≤ 1 QL coverage. Despite being small, such a stretched in-plane lattice constant is obvious and repeatable. We do not know the reason behind this

observation. One might attribute it to the equilibrium lattice constant of an ultrathin Bi_2Se_3 layer that is inherently different from the bulk crystal.^[35] Nevertheless, our preliminary calculations have not provided a strong evidence of such. Further studies are needed to elucidate on the origin of such an observation.

3.2 Bi_2Se_3 deposition on non-vdW substrates

We now turn to discuss the growth properties of Bi_2Se_3 on non-vdW substrates. We have carried out the growth experiment on sapphire (0001), InP(111), GaAs(111), and SiC(0001) of this category. While InP has a lattice constant that closely matches that of Bi_2Se_3 , the others have relatively large lattice misfits, so there is again a strain-relaxation issue. On such substrates, atoms have dangling bonds which may lead to strong chemical interaction between the substrate and Bi_2Se_3 deposit. Taking InP(111)A (indium-terminated face) as an example, each indium (In) atom on surface has an “empty” hybridized bond, which would readily interact with the outmost Se atom having a lone pair orbital. This makes the epitaxy of Bi_2Se_3 on InP to resemble that of covalent semiconductors. The strong chemical interaction between In and Se is verified by first principles calculations.^[20] Such interaction at the heterointerface would make the lattice of Bi_2Se_3 to be strained to that of the substrate for ultrathin layers. Although this is hardly seen for Bi_2Se_3 -on-InP due to the small lattice mismatch, on other substrates of similar character such as GaAs(111)A, we expect strained films to be observable. One notes, however, that as Bi_2Se_3 grows in the unit of one QL, which has a thickness of ~ 1 nm, the strain energy could already be too high to sustain a fully strained Bi_2Se_3 QL on substrates with relatively large lattice misfits.^[36,37] Therefore in general, the films are partially strained. This appears indeed the case as shown in Fig. 4 (crosses and yellow line) recorded during Bi_2Se_3 deposition on GaAs(111)A. Note the seemingly smaller lattice constants of the initially nucleated Bi_2Se_3 islands on GaAs (a substrate having an in-plane lattice parameter of ~ 4 Å) (yellow line and blue crosses). It indicates the nucleated Bi_2Se_3 on GaAs(111) is indeed partially strained. Similar to growth on vdW

substrates, the lattice parameter also evolves with deposition coverage, showing a similar lattice stretch at about 1 QL.

Another interesting observation of Bi_2Se_3 growth on InP(111)A and GaAs(111)A is the diminished twin defects in the epifilms. Fig. 5 shows an example of a surface of Bi_2Se_3 grown on InP(111)A. The surface is again composed of triangular mounds. These mounds are however uniformly oriented towards one and the same direction, suggesting single domain films according to the previous discussions. The LEED measurements show diffraction patterns of three-fold symmetry (Fig. 5 inset), confirming the single domain of the epifilm.^[20]

In passing, we make a comment on the step structure on the mounds. Often, the mounds are spirals with winding steps at the sides, which are caused by preferential growths at dislocations.^[38] Recently a new mechanism has been proposed where a spiral mound forms via growth front pinning followed by an upward climbing of a portion of the pinned growth front over a step.^[39] An examination of the mounds in Fig. 5, however, reveals they are of the wedding-cake structure. The wedding-cake-shaped mounds were previously reported in some other epitaxial systems such as metals and semiconductors^[40, 41] and were attributed to an Ehrlich-Schwoebel barrier.^[42, 43] This observation of the wedding-cake mounds in Bi_2Se_3 calls for a study of surface kinetics of the system in such a direction.

Returning to twin suppression in epitaxial Bi_2Se_3 on InP and GaAs substrates, one might think it is related to strong chemical interaction between the substrate and epitaxial Bi_2Se_3 and so the subsurface layer(s) of the substrate affect the stacking of atoms of epitaxial Bi_2Se_3 . However, total energy calculations comparing the two stacking configurations of one QL Bi_2Se_3 on 6-bilayer InP “substrate”, $[\text{ABCABC}]_{\text{InP}}-[\text{abcab}]_{\text{Bi}_2\text{Se}_3}$ versus $[\text{ABCABC}]_{\text{InP}}-[\text{acbac}]_{\text{Bi}_2\text{Se}_3}$, suggest the two stackings are more or less degenerate, with the rotated stacking being slightly more favorable by $\sim 8 \text{ meV}/(1\times 1)\text{cell}$.^[20] Experimentally, we observe an aligned epitaxial relation, i.e.,

$\text{Bi}_2\text{Se}_3[111] \parallel \text{InP}[111]$ and $\text{Bi}_2\text{Se}_3[\bar{1}\bar{1}2] \parallel \text{InP}[\bar{1}\bar{1}2]$, which is at odd with the calculation. Thus we believe the twin domain suppression in Bi_2Se_3 on InP and GaAs is again to do with a lattice constraint by steps of the substrate. In fact, subsequent experiments on carefully treated substrates with large terraces, where Bi_2Se_3 growth proceeded by island nucleation, resulted in epifilms that were indeed twinned. On the other hand, step-flow growth on vicinal InP substrates consistently produced single domain films.^[20]

In some previous studies, phosphor (P) terminated InP(111)B surface had been adopted as the substrate for Bi_2Se_3 epitaxy.^[19] P atoms on InP(111)B have lone electron pairs, which makes Bi_2Se_3 growth on top of it being vdWe-like. We have examined the formation energy of a Bi_2Se_3 QL on InP(111)B and found an energy cost of 0.489 eV per (1×1) cell over that on InP(111)A.^[20] So despite Bi_2Se_3 grows on InP(111)B, it is less favorable when compared to growth on In-terminated InP(111)A surface. Another promising substrate is CdS, which also has a small lattice misfit with Bi_2Se_3 . Surface atoms of CdS have similar bonding characteristics to InP and so similar growth behaviors may be expected.

Finally, a point worth attention is the terrace-and-step morphology of epitaxial Bi_2Se_3 on vicinal substrates (such as that in Fig. 3). This morphology is typical for step-flow growth of covalent semiconductors and the epifilm and the substrate are thus c -axis parallel (see Fig. 6a), i.e., $\text{Bi}_2\text{Se}_3[111] \parallel \text{InP}[111]$, for example. Such a “coherent” epitaxial relation is however not of the characteristics of van der Waals epitaxy in strict sense. For the latter, one would expect a Bi_2Se_3 film “floats” on the stepped substrate surface, and its c -axis would be parallel to the surface normal (refer to Fig. 6b). The [111] direction of InP substrate and the Bi_2Se_3 epifilm would then differ by an angle θ equal to the offcut angle of the substrate. The fact that this is not the case may again reflect a strong chemical interaction of atoms at steps, preventing such strict vdW processes.

4. High-index Bi₂Se₃ Epitaxy on InP(001) and GaAs(001) substrates

Until recently, studies of 3D topological insulators like Bi₂Se₃, Bi₂Te₃ or Sb₂Te₃ have been exclusively on their hexagonal (111) surfaces. This is mainly because of the ease to achieve such surfaces by cleaving bulk crystals or by epitaxial growths of thin films. Surfaces other than the (111) were not available. Attempts to epitaxially grow TI films along other directions than the *c*-axis existed but were not very successful.^[44-47] In these efforts, non-hexagonal substrate surfaces were naturally adopted in order to facilitate high-index Bi₂Se₃ epilayers. Disappointedly, almost all of the past experiments using, e.g., Si(001),^[44] Al₂O₃(110),^[45] GaAs(001),^[46] and InP(001),^[47] had resulted in (111) films instead.

Recently, Z. J. Xu et al. reported successful growth of a Bi₂Se₃(221) film on purposely treated InP(001) substrate.^[48] ARPES measurements of such a sample revealed not only the Dirac cone structure of the surface electrons but also an elliptical Fermi surface. Correspondingly, magneto-transport studies of such films unveiled anisotropic properties.^[48, 49] Lately, we obtained the same Bi₂Se₃(221) film also on GaAs(001) substrate. Interestingly and importantly, we found the epilayers are fully strained to the lattices of the substrates even for thick layers.

Fig. 7a and 7b present STM micrographs at different length scales of a surface of an epitaxial Bi₂Se₃(221) on InP(001). Note the striped morphology that is distinctly different from the mounded surfaces of Bi₂Se₃(111) films discussed earlier. X-ray diffraction (XRD) and the RHEED measurement unambiguously point to the epilayer to be of Bi₂Se₃(221) with the epitaxial relation of Bi₂Se₃[1 $\bar{1}$ 0]||InP[1 $\bar{1}$ 0], and Bi₂Se₃[11 $\bar{4}$]||InP[110]. This is schematically shown in Fig. 8(a & b).^[48]

We remark that such a high-index film is obtainable only on the specially treated substrates, where the surfaces become roughened containing 3D islands bounded by the {111}

facets. The RHEED show linked spotty patterns (Fig. 7c). Subsequent Bi_2Se_3 deposition at 443 K smoothen the surface and the RHEED pattern becomes streakier (Fig. 7d). We believe $\text{Bi}_2\text{Se}_3(221)$ film results via $\text{Bi}_2\text{Se}_3(111)$ nucleation on the $\{111\}$ facets of the substrate, as schematically illustrated in Fig. 8c. In other words, it is the faceted islands that guide the $\text{Bi}_2\text{Se}_3(221)$ film to grow along the surface normal. This conjecture may be supported by an experimental fact that on a smooth $\text{InP}(001)$ surface without faceted islands, $\text{Bi}_2\text{Se}_3(111)$ film is obtained instead.^[47, 48]

Based on the RHEED and LEED measurements, we further find that epitaxial $\text{Bi}_2\text{Se}_3(221)$ on InP and GaAs substrates are fully strained to the lattices of the substrate along the $\text{Bi}_2\text{Se}_3[11\bar{4}]$ direction. Such strains are huge, amounts to about 9% stretching on InP . This is possible only because along $\text{Bi}_2\text{Se}_3[11\bar{4}]$, there are weakly bonded vdW gaps, as seen from the illustration of Fig. 8b. Such in-plane stretching does not cause out-of-plane compression, however.^[48] The fact that $\text{Bi}_2\text{Se}_3(221)$ can be in-plane strained to large extents by the lattice of the substrate suggests a possibility of probing the strain effect on the properties of TIs,^[50] which will open a new avenue of research in this important field.

5. Conclusion and Perspectives

The layered structure of Bi_2Se_3 makes the compound relatively easy to grow on various substrates by the epitaxial method of MBE. Because of the same reason, however, only $[111]$ oriented films are obtainable on flat substrates irrespective of the symmetry of their surface lattices. For growth on hexagonal symmetrical substrate surfaces, one may still make a distinction between the van der Waals type of substrates and those of non-vdW category, where some differences in growth characteristics are noted. Considering the layered structure of Bi_2Se_3 , one would choose a vdW substrate in order to better accommodate the lattice misfit strain. At the heterointerface, the weak vdW bonding between Bi_2Se_3 and the substrate makes the epifilm

unconstrained by the lattices of the substrate and the epitaxy is incoherent. In other words, the epilayer is fully lattice-relaxed even at the beginning of deposition. It is however surprising to observe a slightly stretched lattice of Bi_2Se_3 at the ~ 1 QL coverage. Despite the ease of strain relaxation, experiments have also indicated an advantage of using a lattice-matched substrate for better epitaxial Bi_2Se_3 , suggesting a role of misfit strain on nucleation of Bi_2Se_3 , which in turn affects defect formation and lattice alignment. Indeed, rotation and twin domains are common in the epilayers of Bi_2Se_3 grown on vdW substrates. On a non-vdW substrate, there exist stronger chemical interactions between atoms of the deposit and the substrate, so the lattices of the latter may play a constraining role to the lattices of the deposit. Firstly, the epilayer is more strained at the beginning stage of deposition. Second, there is also a better alignment of lattices of the deposit to that of the substrate, probably due to a non-negligible effect of substrate subsurface layers on atomic stacking of the deposit and to the chemical bonding at steps. Therefore, a single-domain Bi_2Se_3 film is obtained on $\text{InP}(111)\text{A}$ and $\text{GaAs}(111)\text{A}$. These results form a basis for future searches of substrates for better growth of other layer-structured compounds, including TIs.

Another aspect of TI research is an investigation of surface states on surfaces other than (111). This is encouraged by the recent success of growth of $\text{Bi}_2\text{Se}_3(221)$ films on faceted $\text{InP}(001)$ and $\text{GaAs}(001)$ substrates. We find the $\{111\}$ facets on such substrates guide the growth of high-index $\text{Bi}_2\text{Se}_3(221)$ films in such a way that $\text{Bi}_2\text{Se}_3(111)\parallel\text{InP}(111)$ relation is observed. Importantly, for such epitaxial $\text{Bi}_2\text{Se}_3(221)$ films, because the vdW gaps are now inclined with respect to the surface/interface, they can be tuned by the lattices of the substrate so that the epilayer is fully in-plane strained along one particular crystallographic direction. This leads to a future experimental effort of growing $\text{Bi}_2\text{Se}_3(221)$ on some other (001) substrates for different strains, and if available, the strain effect on TI states can be probed. Secondly, one may also consider choosing other planes of the substrates, such as the (110) plane of InP and GaAs , for growth of Bi_2Se_3 along other high-index directions.

Acknowledgement

We would like to thank many people who have contributed to the project over the years, including H.D. Li, Z.Y. Wang, H.T. He, H.C. Liu, J.N. Wang, N. Wang, Q. Li, M.Y. Yao, L. Miao, D. Qian, J.F. Jia, B. Zao and X.Q. Dai for an incomplete list. We also acknowledge the Research Grant Council (RGC) of Hong Kong Special Administrative Region for its financial support under the General Research Funds (Nos. 706110 and 706111) and the SRFDP and RGC ERG Joint Research Scheme sponsored by the RGC of Hong Kong and the Ministry of Education of China (M-HKU709/12).

References

- [1] Xia Y, Qian D, Hsieh D, Wray L, Pal A, Lin H, Bansil A, Grauer D, Hor Y S, Cava R J and Hasan M Z 2009 *Nat. Phys.* **5** 398
- [2] Hsieh D, Xia Y, Qian D, Wray L, Dil J H, Meier F, Osterwalder J, Patthey L, Checkelsky J G, Ong N P, Fedorov A V, Lin H, Bansil A, Grauer D, Hor Y S, Cava R J and Hasan M Z 2009 *Nature* **460** 1101-U59
- [3] Checkelsky J G, Hor Y S, Liu M H, Qu D X, Cava R J and Ong N P 2009 *Phys. Rev. Lett.* **103** 246601
- [4] Analytis J G, McDonald R D, Riggs S C, Chu J H, Boebinger G S and Fisher I R 2010 *Nat. Phys.* **6** 960
- [5] Zhang G H, Qin H J, Teng J, Guo J D, Guo Q L, Dai X, Fang Z and Wu K H 2009 *Appl. Phys. Lett.* **95** 053114
- [6] Li H D, Wang Z Y, Kan X, Guo X, He H T, Wang Z, Wang J N, Wong T L, Wang N and Xie M H 2010 *New J. Phys.* **12** 103038
- [7] Zhang Y, He K, Chang C Z, Song C L, Wang L L, Chen X, Jia J F, Fang Z, Dai X, Shan W Y, Shen S Q, Niu Q A, Qi X L, Zhang S C, Ma X C and Xue Q K 2010 *Nat. Phys.* **6** 584
- [8] Cheng P, Song C L, Zhang T, Zhang Y Y, Wang Y L, Jia J F, Wang J, Wang Y Y, Zhu B F, Chen X, Ma X C, He K, Wang L L, Dai X, Fang Z, Xie X C, Qi X L, Liu C X, Zhang S C and Xue Q K 2010 *Phys. Rev. Lett.* **105** 076801
- [9] Richardella A, Zhang D M, Lee J S, Koser A, Rench D W, Yeats A L, Buckley B B, Awschalom D D and Samarth N 2010 *Appl. Phys. Lett.* **97** 262104
- [10] Chen J, Qin H J, Yang F, Liu J, Guan T, Qu F M, Zhang G H, Shi J R, Xie X C, Yang C L, Wu K H, Li Y Q and Lu L 2010 *Phys. Rev. Lett.* **105** 176602
- [11] He H T, Wang G, Zhang T, Sou I K, Wong G K L, Wang J N, Lu H Z, Shen S Q and Zhang F C 2011 *Phys. Rev. Lett.* **106** 166805
- [12] Kou X F, He L, Xiu F X, Lang M R, Liao Z M, Wang Y, Fedorov A V, Yu X X, Tang J S, Huang G, Jiang X W, Zhu J F, Zou J and Wang K L 2011 *Appl. Phys. Lett.* **98** 242102

- [13] Li H D, Wang Z Y, Guo X, Wong T L, Wang N and Xie M H 2011 *Appl. Phys. Lett.* **98** 043104
- [14] Wang Z Y, Guo X, Li H D, Wong T L, Wang N and Xie M H 2011 *Appl. Phys. Lett.* **99** 023112
- [15] Taskin A A, Sasaki S, Segawa K and Ando Y 2012 *Phys. Rev. Lett.* **109** 066803
- [16] He L, Xiu F X, Yu X X, Teague M, Jiang W J, Fan Y B, Kou X F, Lang M R, Wang Y, Huang G, Yeh N C and Wang K L 2012 *Nano Lett.* **12** 1486
- [17] Tarakina N V, Schreyeck S, Borzenko T, Schumacher C, Karczewski G, Brunner K, Gould C, Buhmann H and Molenkamp L W 2012 *Cryst. Growth Des.* **12** 1913
- [18] Zhang L, Hammond R, Dolev M, Liu M, Palevski A and Kapitulnik A 2012 *Appl. Phys. Lett.* **101** 153105
- [19] Schreyeck S, Tarakina N V, Karczewski G, Schumacher C, Borzenko T, Brune C, Buhmann H, Gould C, Brunner K and Molenkamp L W 2013 *Appl. Phys. Lett.* **102** 041914
- [20] Guo X, Xu Z J, Liu H C, Zhao B, Dai X Q, He H T, Wang J N, Liu H J, Ho W K, and Xie M H, 2013 *unpublished*
- [21] Analytis J G, Chu J H, Chen Y L, Corredor F, McDonald R D, Shen Z X and Fisher I R 2010 *Phys. Rev. B* **81** 205407
- [22] Wang J, Li H D, Chang C Z, He K, Lee J S, Lu H Z, Sun Y, Ma X C, Samarth N, Shen S Q, Xue Q K, Xie M H and Chan M H W 2012 *Nano Res.* **5** 739
- [23] Zhang H J, Liu C X, Qi X L, Dai X, Fang Z and Zhang S C 2009 *Nat. Phys.* **5** 438
- [24] Hanaguri T, Igarashi K, Kawamura M, Takagi H and Sasagawa T 2010 *Phys. Rev. B.* **82** 081305
- [25] Koma A 1992 *Surf. Sci.* **267** 29
- [26] Koma A 1992 *Thin Solid Films* **216** 72
- [27] He L, Xiu F X, Wang Y, Fedorov A V, Huang G, Kou X F, Lang M R, Beyermann W P, Zou J and Wang K L 2011 *J. Appl. Phys.* **109** 103702

- [28] Song C L, Wang Y L, Jiang Y P, Zhang Y, Chang C Z, Wang L L, He K, Chen X, Jia J F, Wang Y Y, Fang Z, Dai X, Xie X C, Qi X L, Zhang S C, Xue Q K and Ma X C 2010 *Appl. Phys. Lett.* **97** 143118
- [29] Wang Z Y, Li H D, Guo X, Ho W K and Xie M H 2011 *J. Cryst. Growth* **334** 96
- [30] Greenberg J 2001 *Thermodynamic Basis of Crystal Growth: P-T-X Phase Equilibrium and Non-stoichiometry* (Berlin: Springer)
- [31] Bringans R D and Olmstead M A 1989 *Phys. Rev. B* **39** 12985
- [32] Bansal N, Kim Y S, Edrey E, Brahlek M, Horibe Y, Iidad K, Tanimura M, Li G H, Feng T, Lee H D, Gustafsson T, Andrei E and Oh S 2011 *Thin Solid Films* **520** 224
- [33] Meyerson B S, Himpfel F J and Uram K J 1990 *Appl. Phys. Lett.* **57** 1034
- [34] Xie M H, Seutter S M, Zhu W K, Zheng L X, Wu H S and Tong S Y 1999 *Phys. Rev. Lett.* **82** 2749
- [35] Liu F, *private communication*
- [36] Van der merwe J H 1970 *J. Appl. Phys.* **41** 4725
- [37] Matthews J W and Blakeslee A E 1974 *J. Cryst. Growth* **27** 118
- [38] Burton W K, Cabrera N and Frank F C 1951 *Phil. Trans. R. Soc. A* **243** 299
- [39] Liu Y, Weinert M and Li L 2012 *Phys. Rev. Lett.* **108** 115501
- [40] Johnson M D, Orme C, Hunt A W, Graff D, Sudijono J, Sander L M and Orr B G 1994 *Phys. Rev. Lett.* **72** 116
- [41] Stroscio J A, Pierce D T, Stiles M D, Zangwill A and Sander L M 1995 *Phys. Rev. Lett.* **75** 4246
- [42] Ehrlich G and Hudda F 1966 *J. Chem. Phys.* **44** 1039
- [43] Schwoebel R L 1969 *J. Appl. Phys.* **40** 614
- [44] Ferhat M, Liautard B, Brun G, Tedenac J C, Nouaoura M and Lassabatere L 1996 *J. Cryst. Growth* **167** 122
- [45] Tabor P, Keenan C, Urazdhin S and Lederman D 2011 *Appl. Phys. Lett.* **99** 013111
- [46] Liu X, Smith D J, Fan J, Zhang Y H, Cao H, Chen Y P, Leiner J, Kirby B J, Dobrowolska M and Furdyna J K 2011 *Appl. Phys. Lett.* **99** 171903

- [47] Takagaki Y and Jenichen B 2012 *Semicond Sci. Tech.* **27** 035015
- [48] Xu Z, Guo X, Yao M, He H, Miao L, Jiao L, Liu H, Wang J, Qian D and Jia J 2013 *Adv. Mater.* **25** 1557
- [49] He H T, Liu H C, Li B K, Wang J N Guo X, Xu Z J, and Xie M H 2013, *unpublished*
- [50] Liu W L, Peng X Y, Tang C, Sun L Z, Zhang K W and Zhong J X 2011 *Phys. Rev. B* **84** 245105

Figures and captions:

Fig. 1 STM micrograph of a Bi_2Se_3 film grown on Si(111):H substrate (Reprinted from *J. Cryst. Growth* **334**, Z.Y. Wang et al., “Growth characteristics of topological insulator Bi_2Se_3 films on different substrates”, pages 96 – 102 (2011), with permission from Elsevier). The inset shows the LEED pattern (taken at 40 eV) for such a surface, revealing the six-fold symmetry of the lattice.

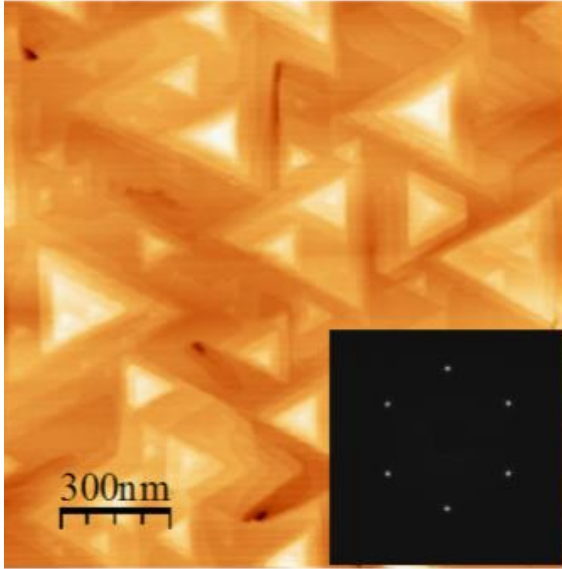


Fig. 2 Stick-and-ball model of a primitive cell of Bi_2Se_3 on a substrate but stacked in different configurations for (a) and (b).

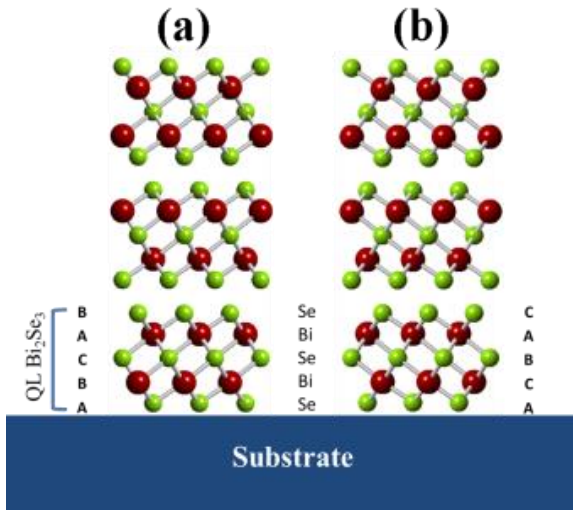


Fig. 3 STM micrograph of a Bi_2Se_3 film grown on a vicinal Si surface (3.5° offcut from (111) towards $[\bar{1}\bar{1}2]$). Inset: a RHEED pattern taken at the early stage of Bi_2Se_3 deposition (electron energy 10 keV, and incident along $\text{Si}[\bar{1}\bar{1}0]$) (Reprinted from *J. Cryst. Growth* **334**, Z.Y. Wang et al., “Growth characteristics of topological insulator Bi_2Se_3 films on different substrates”, pages 96 – 102 (2011), with permission from Elsevier). Note the asymmetric distribution of the spotty diffraction feature signaling a suppression of twin domain in such a film.

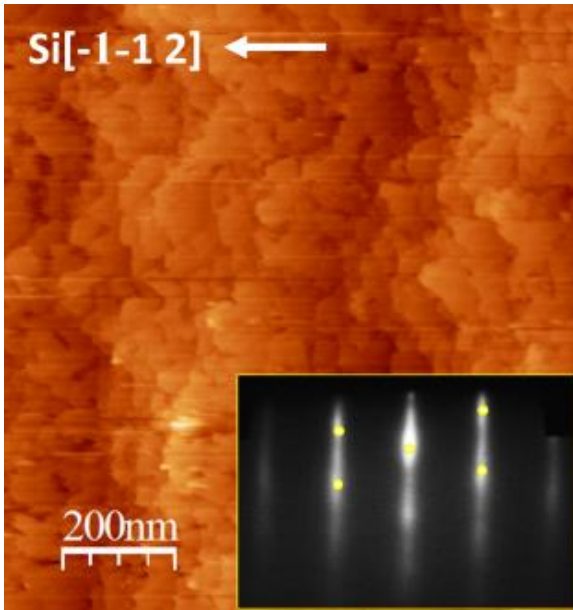


Fig. 4 In-plane lattice constant measured by the RHEED as Bi_2Se_3 depositions proceeded. Red open circles are for growth on $\text{Si}(111):\text{H}$ while blue crosses are for growth on $\text{GaAs}(111)\text{A}$. The superimposed green and yellow lines represent data following 5-adjacent-point-averaging for each case. The horizontal pink line indicates the lattice constant of a strain-free Bi_2Se_3 . The inset shows a RHEED pattern taken at the sub-QL deposition stage of Bi_2Se_3 on $\text{Si}(111):\text{H}$, where two sets of diffraction patterns, one from the substrate and the other from epitaxial Bi_2Se_3 , coexist. The in-plane lattice constants shown in the main figure are derived from the inter-streak spacing D as defined in figure.

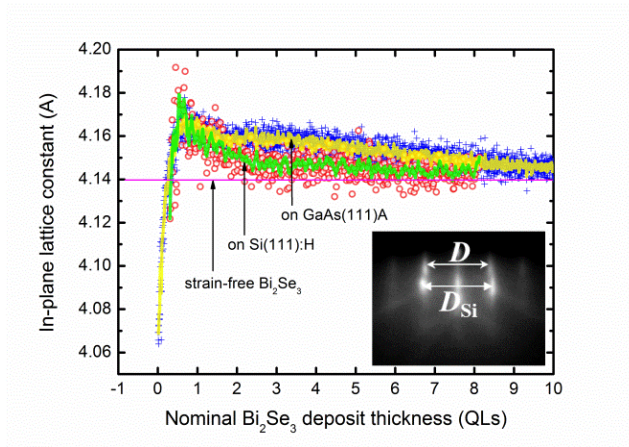


Fig. 5 STM micrograph of a Bi_2Se_3 film grown on $\text{InP}(111)\text{A}$. Note the unidirectional mounds signaling a single domain epifilm, which is further confirmed by the three-fold LEED pattern (taken at the energy of 40 eV) shown in the inset (note the two set of diffraction spots, as marked by “A” and “B” respectively, showing different intensities).

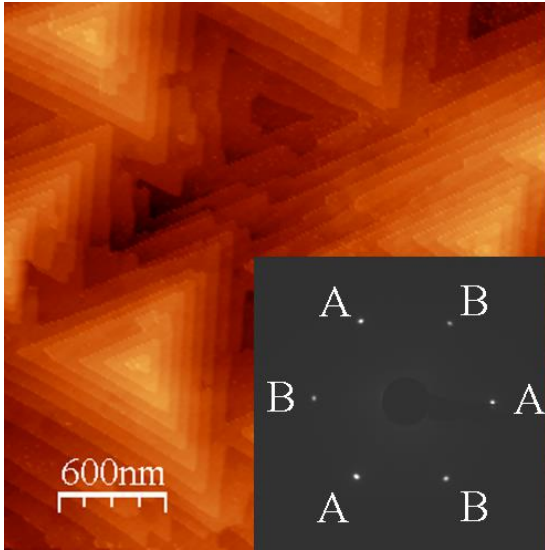


Fig. 6 Schematic illustrations showing (a) “coherent” epitaxial relation and (b) van der Waals epitaxy on a vicinal substrate, such as InP.

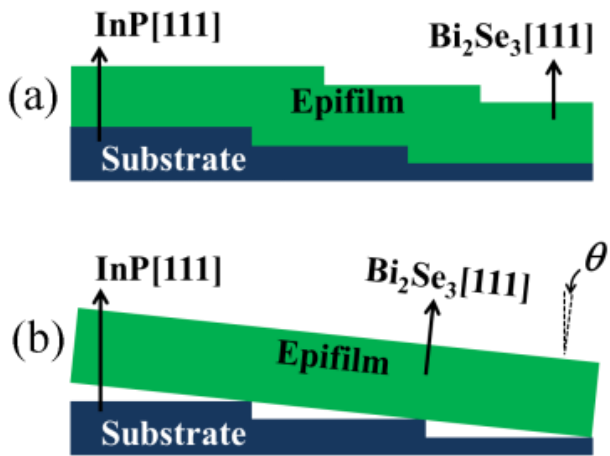


Fig. 7 (a, b) STM micrographs of different length scales of a $\text{Bi}_2\text{Se}_3(221)$ film grown on a nominally flat $\text{InP}(001)$ substrate. (c) RHEED pattern of the substrate following a thermal treatment prior to Bi_2Se_3 deposition. (d) RHEED pattern after Bi_2Se_3 has been grown. For both RHEED experiment, the electron beam energy was 10 keV, and incident along $\text{InP}[\bar{1}\bar{1}0]$ corresponding to the horizontal of the STM image. (Panels **a**, **c** and **d** are reprinted from *Adv. Mater.* **25**, Zhongjie Xue et al., “Anisotropic Topological Surface States on High-Index Bi_2Se_3 Films”, pages 1557 – 1562 (2013), with permission from WILEY).

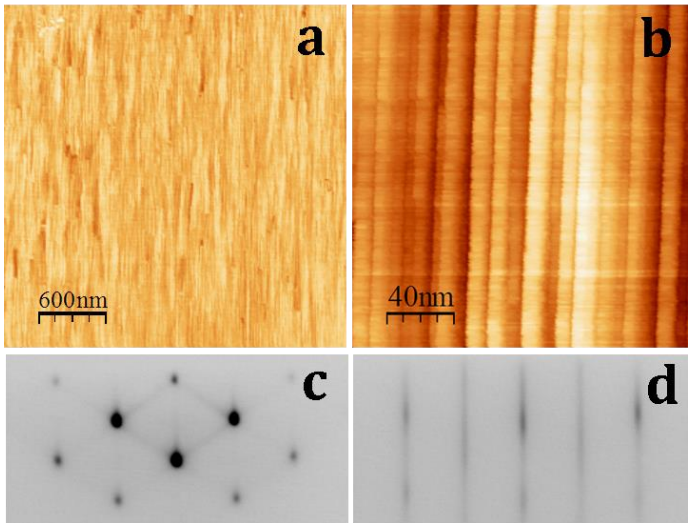


Fig. 8 A model in (a) plan-view and (b) side-view of an epitaxial $\text{Bi}_2\text{Se}_3(221)$ film on $\text{InP}(001)$ substrate (after Ref. [48]). (c) Schematic illustration of $\text{Bi}_2\text{Se}_3(111)$ nucleation and growth as guided by the $\{111\}$ facets of InP , leading to the $\text{Bi}_2\text{Se}_3(221)$ epifilm.

